

FINAL REPORT

OTKA/NKFIH 105622 PD project

TARGETED DRUG DELIVERY ACROSS THE BLOOD-BRAIN BARRIER BY NANOPARTICLES

Papers with acknowledgement of the OTKA/NKFIH 105622 project

1. **Veszélka S**, Mészáros M, Kiss L, Kóta Z, Páli T, Hoyk Z, Bozsó Z, Fülöp L, Tóth A, Rákhely G, Deli MA. Biotin and glutathione targeting of solid nanoparticles to cross human brain endothelial cells. *Curr Pharm Des*. 2017 Jul 27. (2017). IF: 2.86, Q1
2. Dithmer S, Staat C, Müller C, Ku MC, Pohlmann A, Niendorf T, Gehne N, Fallier-Becker P, Kittel Á, Walter FR, **Veszélka S**, Deli MA, Blasig R, Haseloff RF, Blasig IE, Winkler L. Claudin peptidomimetics modulate tissue barriers for enhanced drug delivery. *Ann N Y Acad Sci*. 1397(1):169-184.(2017). IF: 4.52, D1
3. Kovács T, Billes V, Komlós M, Hotzi B, Manzóger A, Tarnóci A, Papp D, Szikszai F, Szinyákovics J, Rácz Á, Noszál B, **Veszélka S**, Walter FR, Deli MA, Hackler L Jr, Alföldi R, Huzian O, Puskas LG, Liliom H, Tárnok K, Schlett K, Borsy A, Welker E, Kovács AL, Pádár Z, Erdős A, Legradi A, Bjelik A, Gulya K, Gulyás B, Vellai T. The small molecule AUTEN-99 (autophagy enhancer-99) prevents the progression of neurodegenerative symptoms. *Sci Rep*. 7:42014. (2017). IF:4.26, D1
4. **Veszélka S**, Bocsik A, Walter F, Hantosi D, Deli MA. Blood-brain-barrier co-culture models to study nanoparticle penetration: focus on co-culture systems. *Acta Biologica Szegediensis* 59:157-168. (2015). Q3

Note: this review was written upon request as part of a University of Szeged – BRC TÁMOP project

Manuscripts in preparation:

1. **Szilvia Veszélka**, András Tóth, Fruzsina R. Walter, Andrea E. Tóth, Ilona Gróf, Mária Mészáros, Alexandra Bocsik, Monika Vastag, Gábor Rákhely, Mária A. Deli. Comparison of a rat primary cell based blood-brain barrier model with epithelial and brain endothelial cell lines: gene expression and drug transport. To be submitted to Journal of Cerebral Blood Flow and Metabolism, IF: 5,07, D1
2. Mária Mészáros, Gergő Porkoláb, Ana-Maria Pilbat, Zsolt Török, Zsolt Bozsó, Albert Kéri, Gábor Galbács, László Siklós, Piroska Szabó-Révész, Mária A. Deli, **Szilvia Veszélka**. Targeted delivery of vesicular nanoparticles across a culture model of the blood-brain barrier. To be submitted to Journal of Nanobiotechnology, IF: 4,94, D1

Introduction

Pharmaceutical treatment of most disorders of the central nervous system (CNS), like neurodegenerative diseases, stroke or brain tumors, is far from satisfactory due to the poor penetration of therapeutic drugs to the brain (Neuwelt et al., 2011). The blood-brain barrier (BBB) is a major obstacle to prevent potential neuropharmaceuticals, especially new biopharmaceuticals, nucleic acids, peptide or protein drugs, to reach their targets in the CNS (Pardridge WM, 2012). The barrier is formed by brain endothelial cells lining the cerebral capillaries, and plays an important role in the homeostatic regulation of the brain microenvironment necessary for the stable and co-ordinated activity of neurons (Abbott et al., 2010). Due to the diversity of neurotherapeutics and the complexity of the BBB functions and regulation of transport systems several strategies and new drug delivery and targeting systems are currently being examined which show great potential future medical application. In the last two decades the potential of nanoparticles (NPs) as drug carriers including vesicular and solid NPs is increasingly investigated for drug delivery across the BBB. While the receptor-mediated transport systems of brain endothelial cells have been investigated as a way of drug delivery across the BBB for several decades (Pardridge, 2012) other physiological pathways, especially the nutrient carrier systems of the BBB have been studied only recently for CNS delivery (Pardridge WM, 2015). In contrast to NPs for CNS delivery targeted by antibodies or peptides there are only few papers describing NPs labeled with ligands of nutrient transporters present at the BBB. Targeting tight junctional proteins of brain endothelial cells is another strategy for drug delivery via transient opening of the BBB (Bocsik et al. 2016). To increase the efficiency of drug targeting to the brain in our project we tested both strategies.

Aims

To test the uptake and permeability of solid and vesicular nanoparticles targeted with biotin, alanin, glutathione or their combinations as ligands of nutrient transporters at the BBB. To elucidate certain elements of the transport mechanism of targeted nanoparticles in brain endothelial cells. To explore the gene expression of nutrient transporters in brain endothelial cells as possible targets of functionalized nanoparticles. To target the interendothelial junction proteins of brain endothelial cells to increase the uptake of therapeutics via transient BBB opening.

1. Results with solid nanoparticles

We designed solid nanoparticles (SNP) labeled with transporter ligands to test them as BBB targeting vectors. The commercially available solid fluorescent particles (TransFluoSpheres Fluorescent Microspheres, Thermo Fisher Scientific Inc.,) were already functionalized with neutravidin. These neutravidin-coated particles were labeled with biotin and biotinylated-glutathione (for schematic drawing see Fig. 1).

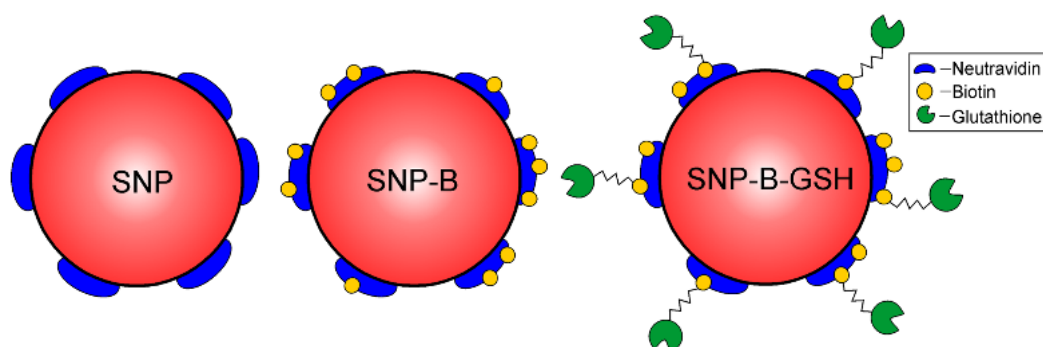


Fig. 1. Schematic drawing of non-targeted (SNP), biotin- (SNP-B) and glutathione-labeled (SNP-B-GSH) solid nanoparticles.

All SNPs had low polydispersity index, indicating a relatively narrow size distribution. The average zeta potential for both targeted particles was very similar. The charge of the non-labeled SNP was less negative (**Table1**).

Table 1. Characterization of the non-targeted and targeted solid nanoparticles

Nanoparticle	Size (nm)	Polydispersity index	Zeta potential (mV)
SNP	93 ± 0.59	0.131 ± 0.02	-14 ± 0.87
SNP-B	118.1 ± 2.9	0.251 ± 0.001	-23.1 ± 0.62
SNP-B-GSH	120.5 ± 2.86	0.261 ± 0.01	-23.8 ± 1.33

Values presented are means ± SD. SNP, non-targeted solid nanoparticles; SNP-B, biotin-targeted solid nanoparticles; SNP-B-GSH, glutathione-targeted solid nanoparticles.

The morphology of the nanoparticles was observed by scanning electron microscopy (Fig. 2). The particles had mostly spherical shapes, but some SNPs were elongated. No aggregation was visible.

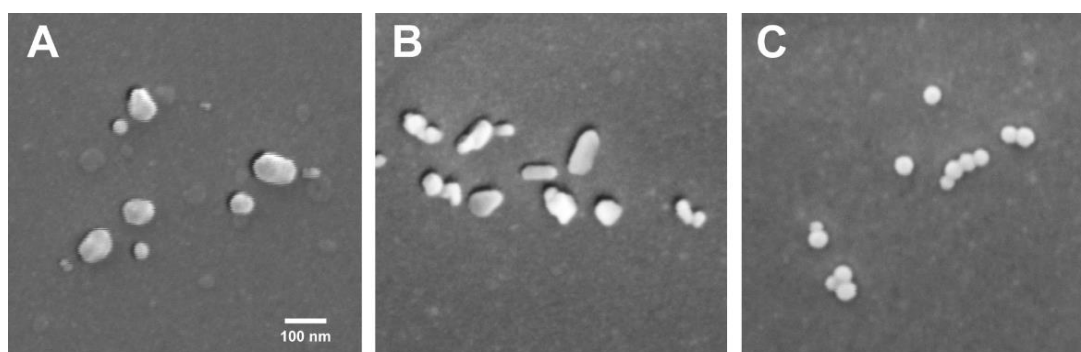


Fig. 2. Scanning electron microscopy images of non-targeted (A), biotin-targeted (B), and glutathione-targeted (C) solid nanoparticles. Bar: 100 nm

Effect of SNPs on the cell viability of brain endothelial cells

Incubation of the hCMEC/D3 human brain endothelial monolayers with SNP and SNP-B for 24 hours had no effect on cell viability assessed by MTT dye conversion assay (Fig. 3). SNP-B-GSH increased the metabolic activity of cells at 30-100 $\mu\text{g}/\text{mL}$, while the highest concentration caused a reduction in viability. For further experiments the 150 $\mu\text{g}/\text{mL}$ concentration was selected for all three SNPs, which can be considered as non-toxic.

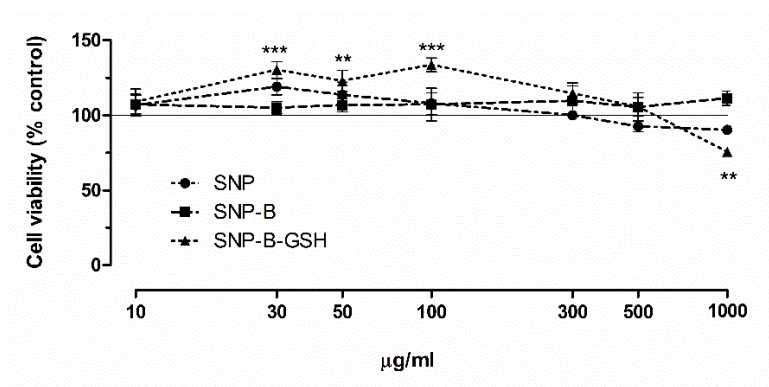


Fig. 3. The effect of non-targeted (SNP), biotin-targeted (SNP-B), and glutathione-targeted (SNP-B-GSH) solid nanoparticles on the viability of brain endothelial cells (24 hours). Values presented are means \pm SEM. Statistical analysis: one-way analysis of variance followed by Dunnett's posttest, ** $P < 0.01$; *** $P < 0.001$ compared to control. $n = 4-8$. X-axis: log-10 scale.

Uptake of SNPs in brain endothelial cells

After 4 hours of incubation no significant difference between the uptakes of three SNPs in brain endothelial cells could be measured, although an increasing trend was seen in case of targeted SNPs (Fig. 4).

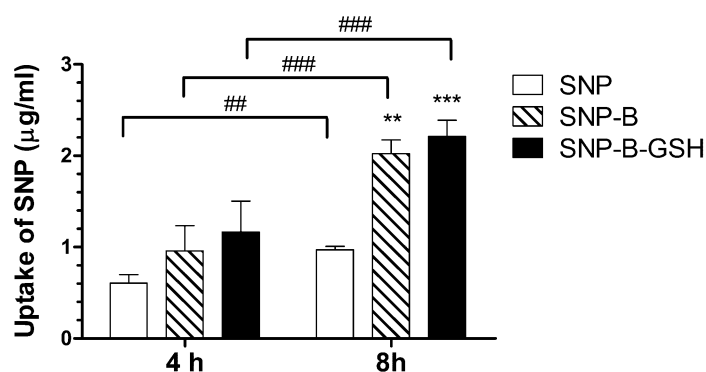


Fig. 4. The uptake of non-targeted (SNP), biotin-labeled (SNP-B) and glutathione-labeled (SNP-B-GSH) solid nanoparticles in brain endothelial cells after 4 or 8 hours incubation. The concentration of SNPs is 150 $\mu\text{g}/\text{mL}$ in each groups. Values presented are means \pm SEM. Statistical analysis: two-way analysis of variance followed by Bonferroni posttest, where ** $P < 0.01$; *** $P < 0.001$, compared to SNP treated group, ## $P < 0.01$; ### $P < 0.001$, compared to the 4 hour-incubation group; $n = 4-6$.

After 8-hour incubation the uptake of all tested nanoparticles was significantly higher compared to the 4-hour group. Importantly the uptake of the biotin- and glutathione-targeted SNPs was significantly increased; it was two times higher than the uptake of the non-targeted particle. The uptake of the fluorescent nanoparticles could be visualized in brain endothelial cells by confocal microscopy (Fig. 5). Red fluorescent dots can be seen in the cytoplasm of the cells treated with SNPs. More fluorescent particles were seen in cells incubated with glutathione-labeled SNPs indicating better uptake of these nanoparticles as compared to the non-targeted SNPs.

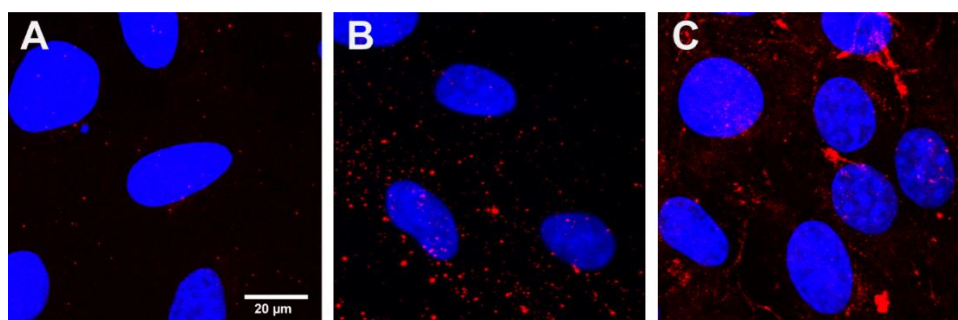


Fig. 5. Confocal microscopy images of cultured human brain endothelial cells incubated with non-labeled (A), biotin-labeled (B), and glutathione-labeled (C) solid nanoparticles (red) for 8 hours at 37 °C. The concentration of SNPs was 150 µg/mL in each groups. Cell nuclei were stained with bis-benzimide (blue). Bar: 20 µm.

Penetration of SNPs across brain endothelial monolayers

The permeability of hCMEC/D3 brain endothelial cell monolayers for Evans blue-albumin was $1.6 \pm 0.3 \times 10^{-6}$ cm/s which reflects a suitable barrier for testing SNPs. All SNPs crossed the brain endothelial layers in the permeability tests but at different extent (Fig. 6). After 8-hour incubation the P_{app} of biotin targeted SNP was 2.8 fold higher than that of the non-targeted SNP. The penetration of the glutathione targeted nanoparticles was the highest, a significant, 5.8 fold increase was measured as compared to the unlabeled SNP group.

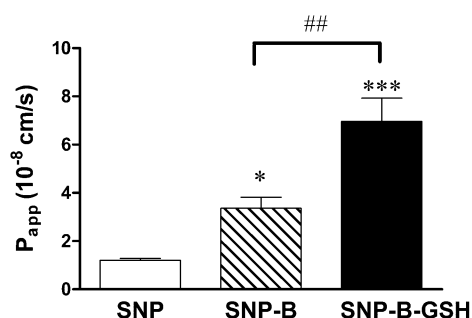


Fig. 6. Permeability changes of brain endothelial monolayers after SNP treatments (150 µg/mL, 8 h). Values presented are means \pm SEM. Statistical analysis: one-way analysis of variance followed by Bonferroni posttest. * $P < 0.05$, *** $P < 0.001$, compared to non-labeled SNP treated group; ## $P < 0.01$, compared to biotin-labeled SNP treated group, $n = 6$.

Expression of SMVT/SLC5A6 mRNA in brain microvessels and cultured brain endothelial cells

We verified, that mRNA of SMVT/SLC5A6 vitamin transporter responsible for shuttling biotin across the BBB, was expressed in isolated rat brain microvessels, and both in hCMEC/D3 human brain endothelial cell line and primary rat brain endothelial cells (Fig.7).

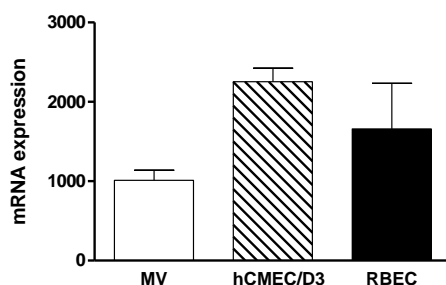


Fig. 7. The expression level of SMVT/SLC5A6 vitamin transporter gene mRNA in isolated rat brain microvessels (MV), hCMEC/D3 human brain endothelial cell line and primary rat brain endothelial cells (RBEC). No statistically significant change (one-way ANOVA and Bonferroni posttest).

2. Results with vesicular nanoparticles

In our second set of experiments non ionic surfactant based vesicular nanoparticles (niosomes; NS) were prepared, targeted with ligands and loaded with Evans blue labeled bovine serum albumin (EBA; 67 kDa) as a model molecule. First Span 60 (sorbitan-monostearate) and Solulan C24 (cholesteryl-poly-24-oxyethylene-ether) and cholesterol were dissolved in hot 1:2 mixtures of chloroform and ethanol in a round-bottom flask. Pegylated-GSH or dodecanoil-alanine (A) were added (5% of total lipids) to prepare the targeted niosomes (NS-GSH or NS-A). For double targeted niosomes the content of ligands was 4-4 % of the total lipids. Two types of glucose analogs, the lipid soluble N-palmitoylglucoseamine and the hydrophilic glucopyranose were also tried as targeting ligands. The removal of the organic solvent by vacuum pump yielded a thin lipid film layer. The dry lipid film was hydrated with phosphate buffer containing EBA. The mixture was heated in a water bath at 40°C for 30 minutes and sonicated for 25 minutes. The suspension was forced through a polycarbonate filter (100 nm pore size) by lipid extrusion technique to yield large, unilamellar vesicles.

Table 2. Characterization of the non-targeted and targeted vesicular nanoparticles.

Nanoparticle	Size (nm)	Polydispersity index	Zeta potential (mV)	Entrapping efficiency (%)
NS	110.4 ± 1.7	0.168 ± 0.005	-3.47 ± 0.6	5.23
NS-A	90.0 ± 0.5	0.187 ± 0.010	-4.69 ± 0.6	4.84
NS-GSH	102.7 ± 0.6	0.164 ± 0.013	-7.56 ± 0.9	3.39
NS-A-GSH	97.7 ± 0.7	0.180 ± 0.012	-6.63 ± 0.9	9.27

Values presented are means ± SD. NS, non-targeted niosomes; NS-A, alanin-targeted niosomes; NS-GSH, glutathione-targeted niosomes, NS-A-GSH, alanin/glutathione-targeted niosomes.

The non entrapped EBA was removed by ultracentrifugation (123 249 g, 6 hours). **Table 2** summarizes the main physicochemical characteristics of the untargeted and targeted niosomes.

Effect of niosomes on the cell viability of brain endothelial cells

Incubation of the primary rat brain endothelial monolayers with NS, NS-A and NS-A-GSH niosomes in the 0.3-10 mg/mL concentration range for 24 hours had no effect on cell viability assessed by impedance measurement except of NS-GSH (Fig. 8). NS-GSH at the highest concentration decreased viability at the end of 24-hours incubation time (Fig. 8). For further experiments with shorter (4 and 8 hours) incubation time we selected the 10 mg/mL concentration for all three groups. N-palmitoylglucoseamine labeled niosomes significantly reduced cell viability, therefore it was excluded from further cell assays.

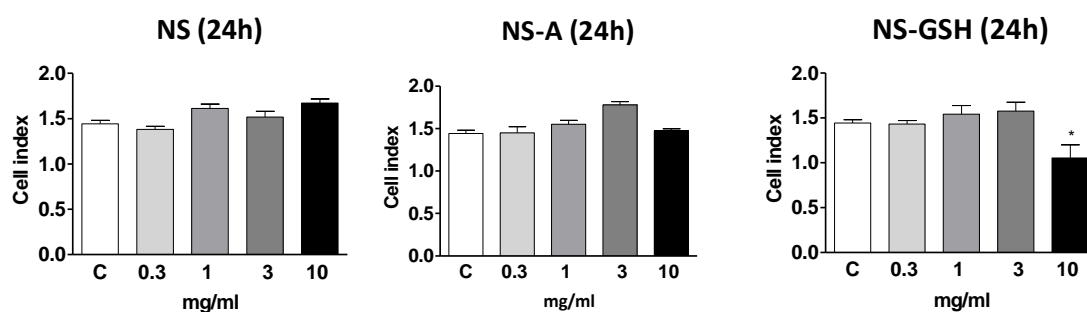


Fig. 8. The effect of non-targeted (NS), alanin-targeted (A), and glutathione-targeted (GSH) niosomes on the viability of brain endothelial cells (24 hours). Values presented are means \pm SEM. Statistical analysis: one-way ANOVA, Dunnett's posttest. * $P < 0.5$ compared to the control groups.

Uptake of niosomes in brain endothelial cells – temperature dependence and metabolic inhibition

Glucopyranose increased the uptake of EBA in vesicles-treated brain endothelial cells, but less efficiently as other ligands. The uptake of single and double targeted niosomes in endothelial cells was tested at two different temperature (Fig. 9A). After 8-hour incubation at 37 °C the uptake of glutathione targeted niosomes (NS-GSH) was significantly higher compared to the non targeted groups (NS) and elevated uptake was seen in case of all other targeted niosomes (Fig. 9A). Importantly the uptake of all tested niosomes was significantly decreased at 4 °C indicating an active transport mechanism of the particles. The metabolic inhibitor sodium azide significantly decreased the uptake of both non-targeted and targeted nanocarriers suggesting an active, energy-dependent uptake process (Fig. 9A). The uptake of EBA, the fluorescent cargo of the nanovesicles was visualized in brain endothelial cells by confocal microscopy (Fig. 9B). A quick acid stripping was performed to remove cell surface associated niosomes similarly to the other uptake assays. Red fluorescent dots were detected in the cytoplasm of the cells treated with double targeted niosomes NS-A-GSH indicating uptake of the cargo. No red fluorescence was seen in the non-targeted NS group.

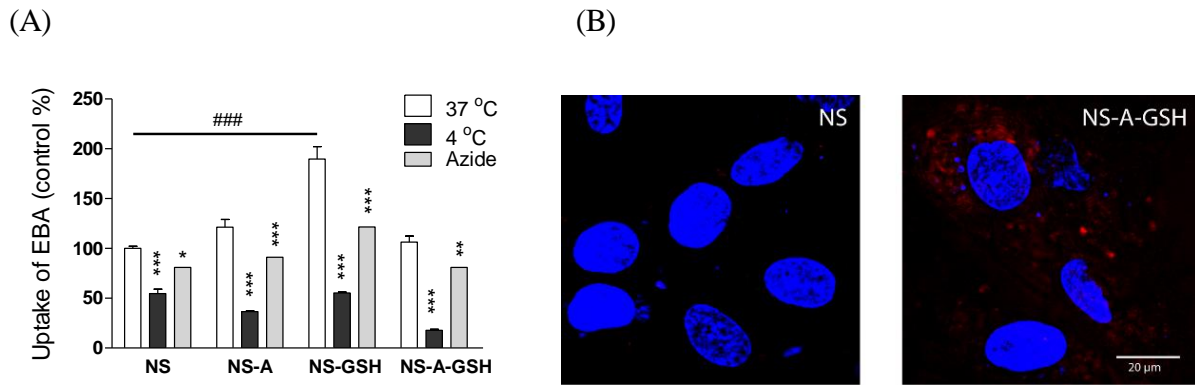


Fig. 9. (A) The effect of temperature and metabolic inhibitor sodium azide (0.1%) on the uptake of non-targeted (NS), alanin-labeled (NS-A), glutathione-labeled (NS-GSH) and alanin/glutathione-labeled (NS-A-GSH) niosomes in brain endothelial cells after 8 hours incubation. The concentration of niosomes was 10 mg/mL in each groups. Values presented are means \pm SEM. Statistical analysis: two-way ANOVA, Bonferroni posttest. * $P < 0.5$; ** $P < 0.01$; *** $P < 0.001$, compared to first column of each groups, ### $P < 0.001$, compared to NS treated group; $n = 4-6$. (B) Confocal microscopy images of cultured human brain endothelial cells incubated with non-labeled (NS) and alanin/glutathione-labeled (NS-A-GSH) niosomes (red) for 8 hours at 37 °C. The concentration of niosomes was 10 mg/mL in both groups. Cell nuclei were stained with bis-benzimide (blue). Bar: 20 μ m

For transmission electron microscopy niosomes with the electron dense lanthanum nitrate (433 Da) as a cargo were prepared. The particles were non toxic and their physicochemical properties were similar to the EBA filled niosomes. The cells were treated with free lanthanum (LA), lanthanum entrapped non-targeted niosomes (NS) and vesicles labeled with double ligands containing lanthanum (NS-A-GSH) for 8 hours. The concentration of lanthanum was equal in each groups (0.2 μ g/mL). More black dots can be seen in the cytoplasm of the cells treated with NS-A-GSH compared to the NS and LA groups indicating better uptake of BBB targeted nanoparticles (Fig. 10).

The presence of lanthanum in the subcellular compartments will be verified by element analysis with a novel instrument soon to be installed in BRC (JEOL JEM-1400PLUS, Energy Dispersive X-ray Spectrometry).

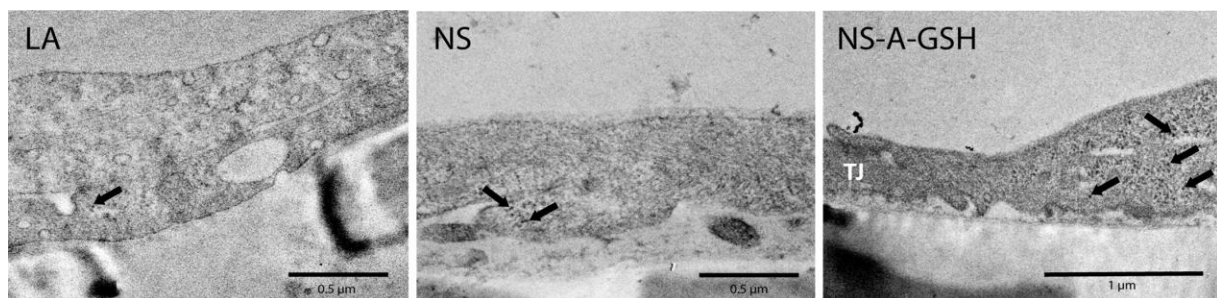


Fig. 10. Transmission electron microscopy images of the uptake of free lanthanum (LA) and lanthanum encapsulated in non-labeled (NS) or alanin/glutathione-labeled (NS-A-GSH) niosomes in brain endothelial cells after 8 hours incubation. Bar: 0.5 and 1 μ m. Arrows: lanthanum dots.

Mechanism of niosome uptake in brain endothelial cells – inhibition of endocytosis

To further elucidate the mechanism of niosome uptake the effect of endocytosis inhibitors was studied using double targeted NS-A-GSH labeled particles. Filipin is the inhibitor of lipid raft/caveolae-mediated endocytosis. It disrupts the structure and functions of the cholesterol-rich membrane domains, which include aberrations in the caveolar shape. Cytochalasin-D, the F-actin-depolymerizing drug blocks membrane ruffling and inhibits macropinocytosis and phagocytosis. Since actin cytoskeleton regulates different endocytic pathways cytochalasin-D is a common inhibitor of endocytosis. Both drugs induced a significant partial inhibition of the uptake of NS-A-GSH niosomes during 4 hours incubation (Fig. 11). These results indicate that endocytosis contributes to the cellular uptake of targeted niosomes. We plan further experiments to identify the subcellular compartments (early and late endosomes, Golgi, lysosomes) where the cargo of niosomes is localized.

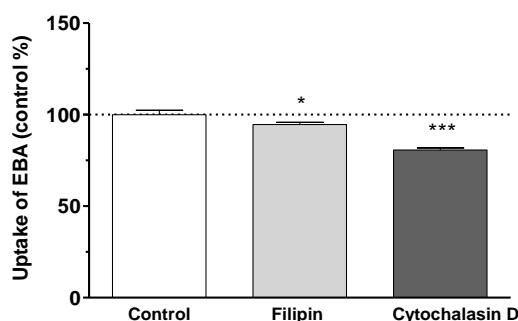


Fig. 11. Inhibition of the uptake of NS-A-GSH niosomes with filipin (6 μ M) and cytochalasin-D (20 μ M) in rat brain endothelial cells (4 hours incubation). The concentration of niosomes was 10 mg/mL in all groups. Values presented are means \pm SEM. Statistical analysis: ANOVA, Dunnett posttest, where * $P < 0.5$; *** $P < 0.001$, compared to the control group; n=6

Mechanism of niosome uptake in brain endothelial cells – measurement of plasma membrane fluidity

We have previously demonstrated, that non-ionic surfactants increase the plasma membrane fluidity of living cells (Kiss et al. 2014). We hypothesized that niosomes may also increase the membrane fluidity of brain endothelial cells indicating fusion of the nanovesicles with the plasma membrane. The membrane fluidity of living brain endothelial cells was determined by the measurement of fluorescence anisotropy of the cationic membrane probe TMA-DPH (1-(1-(4-trimethylammoniumphenyl)-6-phenyl-1,3,5-hexatriene p-toluenesulfonate).

As expected, after 4 hours treatment the anisotropy significantly decreased both in NS and NS-A-GSH treated cells (Fig. 12) indicating increased cell membrane fluidity and a fusion process. The positive control membrane fluidizer benzyl alcohol (30 mM) quickly and greatly reduced the TMA-DPH fluorescence anisotropy after 3 min compared to the control and niosome treated groups.

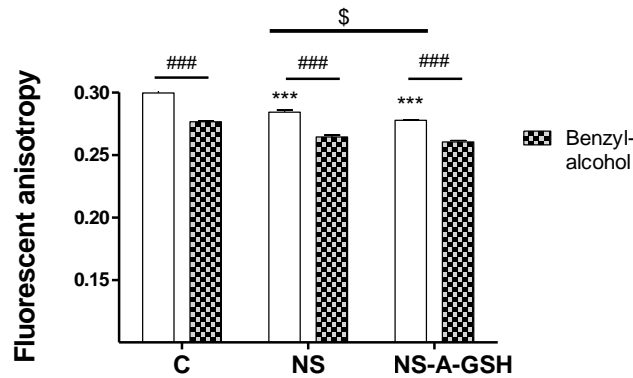


Fig. 12. The effect of niosomes and benzyl alcohol (30 mM) on plasma membrane fluidity measured by TMA-DPH (0.2 μ M) fluorescence anisotropy on living brain endothelial cell suspensions. Data are presented as mean \pm SEM, n = 3; statistical analysis: two-way ANOVA, Bonferroni test; *** P < 0.001, all groups were compared to non treated control (C); ### P < 0.001, compared to first column of each groups; $^{\$}$ P < 0.5 non-targeted NS compared to NS-A-GSH group.

Mechanism of niosome uptake in brain endothelial cells – cell surface charge modification

Several specific features of the BBB limit the penetration of drugs to CNS. Intercellular junctions and drug efflux pumps are widely investigated, but the role of the surface charge of brain endothelial cells in CNS drug delivery is rather unexplored. This highly negative surface charge is composed of the negatively charged lipids in the cellular plasma membrane and the glycocalyx at the luminal surface. The glycocalyx is a 0.1-1 μ m thin layer covering the entire surface of endothelial cells and composed of proteoglycans and glycosaminoglycans (Hervé et al. 2008). The negative surface charge of brain endothelial cells can be measured by zeta-sizer and was found to be the highest among vascular endothelial cells (Ribeiro et al. 2012).

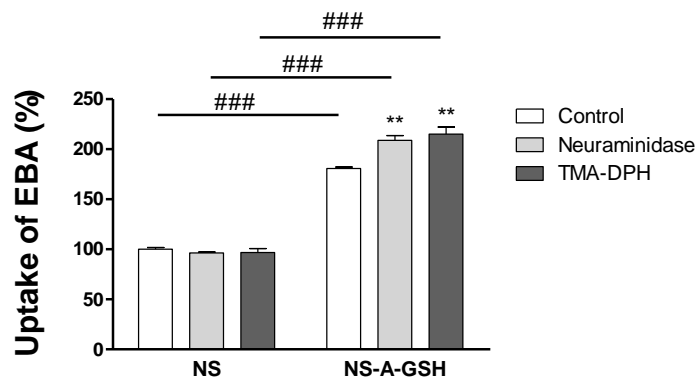


Fig. 13. The effect of neuraminidase (1 U/ml) and TMA-DPH (30 mM) on the uptake of non-targeted (NS) and alanin/glutathione targeted niosomes (NS-A-GSH) in brain endothelial cells. Data are presented as mean \pm SEM, n = 6; statistical analysis: two-way ANOVA, Bonferroni test; ** P < 0.01 compared to first column of each groups; ### P < 0.001, compared to NS treated groups.

This electrostatic barrier may influence the transport of substances and also nanoparticles across the BBB, but the correlation between brain endothelial surface charge and permeability for nanoparticles was not measured and established experimentally yet. We modified the surface

charge of cultured brain endothelial cells by digestion of the glycocalyx with neuraminidase enzyme, or treatment with cationic lipid TMA-DPH and measured the effect on the uptake of niosomes in primary rat brain endothelial cells (Fig. 13). Both treatments made the surface charge of brain endothelial cells more positive, which we verified with zeta potential measurements. Both modifications increased the uptake of targeted niosomes, but brain endothelial surface charge alteration did not affect the cellular uptake of non-targeted nanoparticles (Fig. 13). These new observations indicate, that surface charge at the BBB is important in the uptake mechanism of charged nanoparticles and can be modulated by modification of plasma membrane lipid composition or the glycocalyx.

Penetration of the cargo of targeted niosomes across BBB culture model

The permeability of rat primary brain endothelial cell monolayers for non-encapsulated Evans blue-albumin was $0.2 \pm 0.03 \times 10^{-6}$ cm/s reflecting a suitable tight barrier for testing nanoparticles, in accordance with our previous results (Bocsik et al. 2016). The presence of single and double targeting ligands significantly increased the apparent permeability coefficients (P_{app}) of EBA across the BBB model as compared to the non-targeted NS (Fig. 14). In the BBB permeability measurements the amount of EBA cargo that crossed brain endothelial cells was increased 570 fold in case of the double targeted niosome as compared to the unencapsulated EBA.

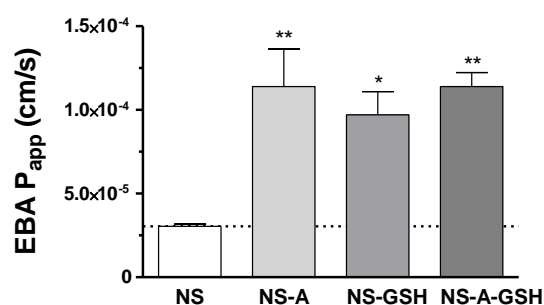


Fig. 14. Permeability changes of brain endothelial monolayers after niosomes treatments (10 mg/mL, 4 h). Values presented are means \pm SEM. Statistical analysis: ANOVA, Bonferroni posttest. * $P < 0.05$, ** $P < 0.01$, compared to non-labeled NS group; n = 4.

Expression of selected genes coding nutrient transporters in primary brain endothelial cell based BBB model and brain endothelial cell lines

In the *in vitro* part of our project both hCMEC/D3 human brain endothelial cell line (D3: hCMEC/D3 cells, D3L: hCMEC/D3 cells improved by lithium treatment; Weksler et al. 2013) and rat brain endothelial cell based co-culture model (EPA: primary brain endothelial cells co-cultured with pericytes and astroglia) were used for the uptake and transport experiments. We verified the expression level of the transporters for the tested targeting ligands on these models (Fig. 15.), except for glutathione, for which the transporter is only functionally identified, but is molecularly unknown (Gaillard et al. 2014). In addition we tested other rat brain endothelial

cell lines (GP8, RBE4), since they are widely used for testing drug and nanoparticle permeability, but no comparative data are available on their transporter expression levels.

The glucopyranose tested in our early experiments, as described in our interim reports, targets glucose transporters. Among these GLUT1 was in both the EPA and D3 models expressed at the highest level (Fig. 15). GLUT1 and -3 were also well expressed in the other four cell line, with the exception of GLUT3 in GP8 cells. The expression level of GLUT5 was low in all tested endothelial models, and not expressed in RBE4 cells.

From the 7 amino acid transporters examined the highest expression level was measured for SAT2, which transports alanine (Campos-Bedolla et al. 2014). CAT1 and LAT1 mRNA were also expressed at high levels in all models.

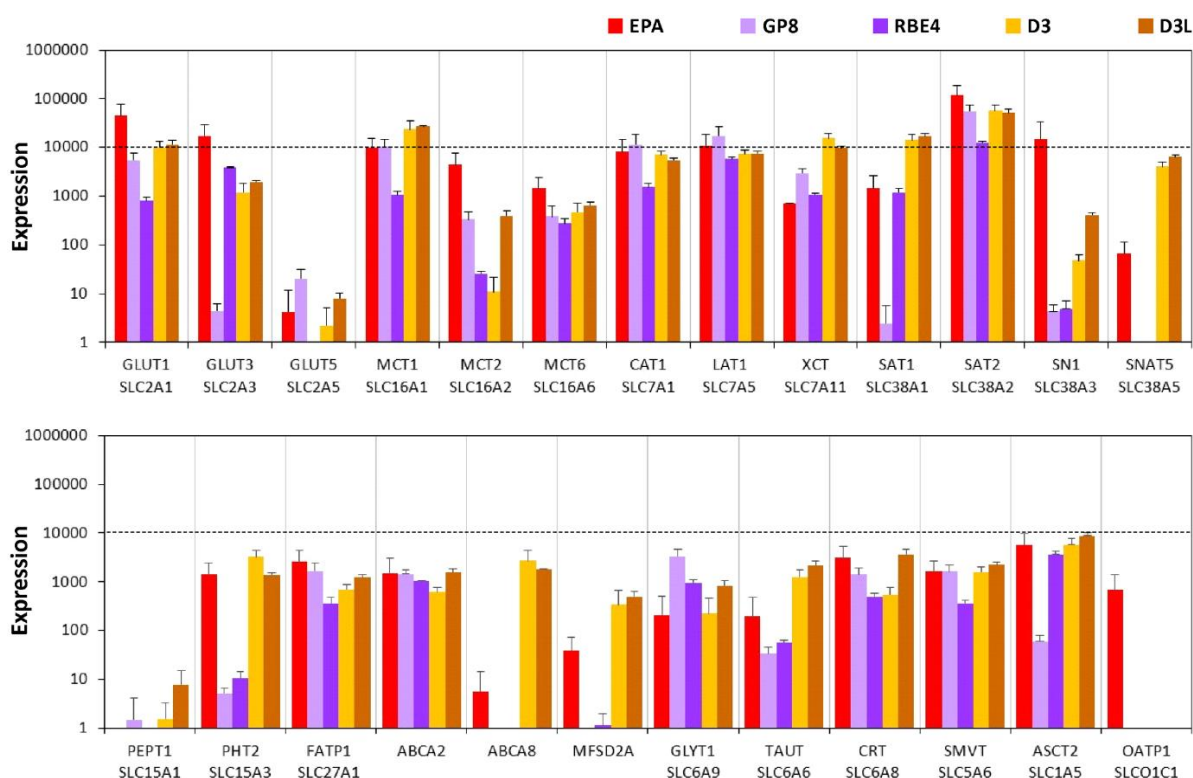


Fig. 15. Expression of selected genes coding solute carrier and other nutrient transporters in a primary rat brain endothelial cell based BBB model (EPA) and in other brain endothelial cell lines (GP8, RBE4, D3 and D3L).

The monocarboxylic acid carrier MCT1 and the amino acid transporter SN1 were also well expressed in the EPA model and could be potential targets of novel functionalized nanoparticles. All other nutrient transporters were expressed at lower, moderate or low levels.

In vivo imaging of targeted niosomes by Explore Optix

Brain penetration of alanin and glutathione-labeled niosomes were tested in mice in cooperation with our German partners (University of Göttingen, Germany). Explore Optix (General Electric, USA), a small animal time-domain pre-clinical imager was used to optical imaging in a non invasive way. This instrument allowed to visualize the nanoparticle biodistribution in real-time and over time in the same animal. Nude male mice were anesthetized by sevoflurane to provide continuous anesthesia during the experiment. Non-targeted, alanin and glutathione, or double NS-A-GSH targeted niosomes containing EBA were tested. EBA or EBA encapsulated in different niosomes were injected intravenously (tail vein). Animals were continuously monitored in the first one hour and later at selected time points. The red fluorescent signal of EBA was detected over the whole body of living anesthetized mice by the *in vivo* optical imaging system (Fig. 16.). The animals were returned to their cage and provided access to food and water between the measurement points.

In the first 1 hour there was no significant accumulation of fluorescent signal in EBA or ligand free, non-targeted EBA-filled niosomes injected mice (Fig. 17.), but after 6 hours fluorescent signal was observed in the liver, but not in the brain.

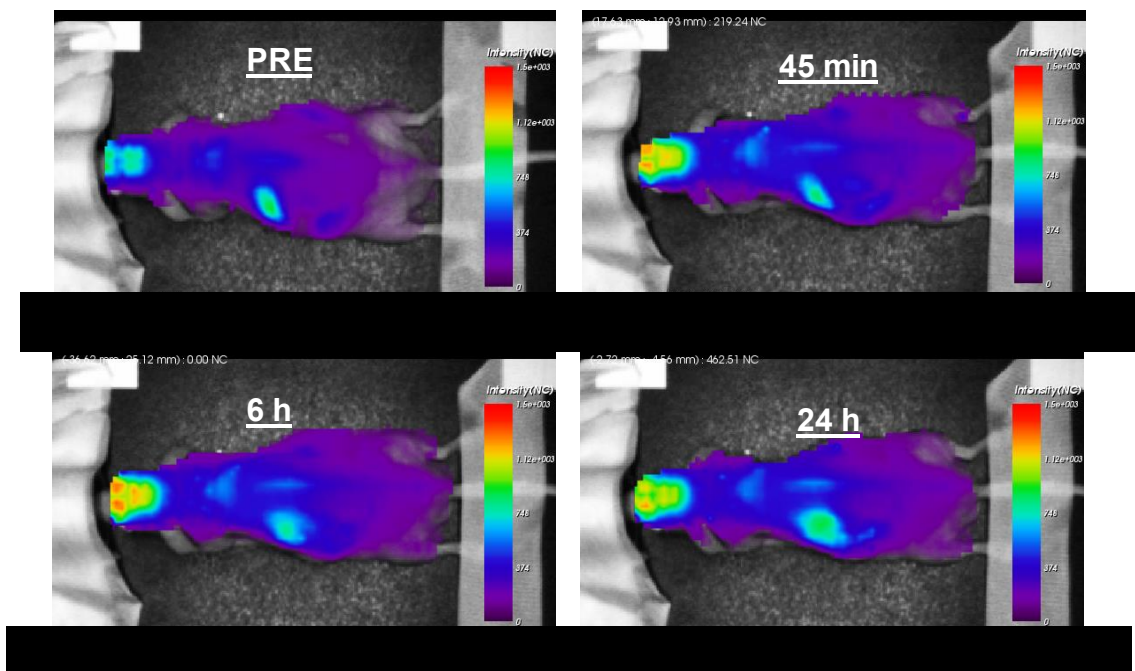


Fig. 16. Explore Optix optical imaging of the distribution of double targeted niosomes after 45 min, 6 h and 24 h of the tail vein injection of nanoparticles in nude mice.

In contrast in mice injected with niosomes labeled with glutathione or alanin as transporter ligands higher fluorescent signal particularly in the brain starting from 1 hour and lasting until 24 hour were measured by *in vivo* imaging (Fig. 16. and 17.).

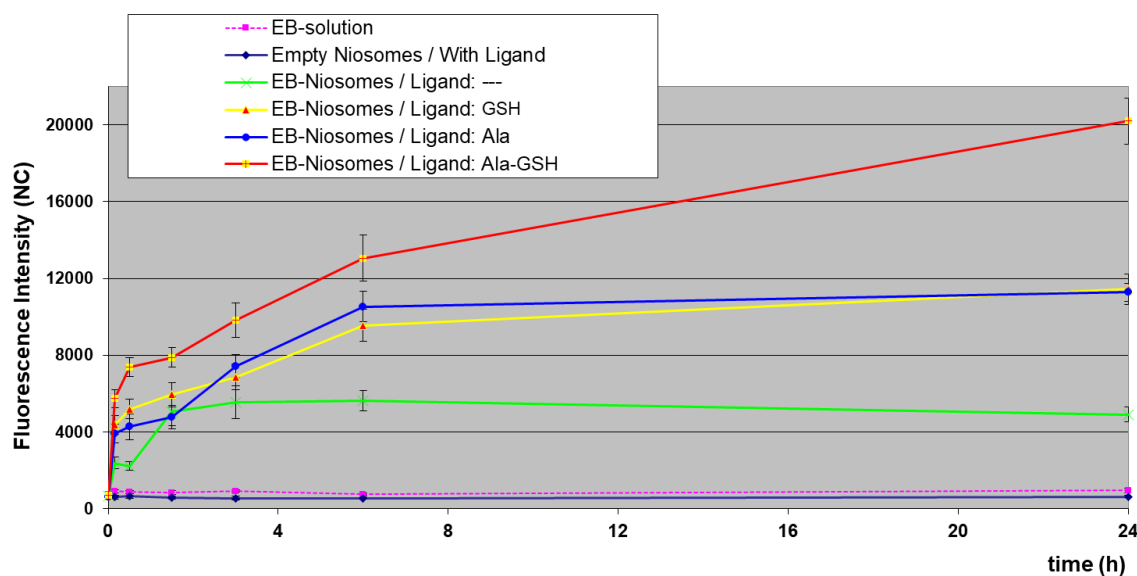


Fig. 17. The fluorescent signal in the brains was significantly increased in alanin/glutathione-labeled niosome compared to EB solution treated, non-labelled niosome or single labeled niosome treated groups scanned by Explore Optix optical imaging.

To verify the organ distribution of the cargo EBA animals were sacrificed by ketamine/xylazine deep anesthesia at 1 and 24 hour time points and after a brief cardiac perfusion with saline organs were dissected and scanned by Explore Optix. The fluorescent signal in the brains *ex vivo* was significantly increased in the glutathione and alanin labeled niosome treated groups at both timepoints. These results indicate that glutathione and alanin as targeting ligands on nanoparticles increase the brain delivery of the albumin cargo, a model molecule for biotherapeutics.

3. Targeting the interendothelial junction proteins of brain endothelial cells

Our team has previously described in a comparative study, that the paracellular cleft between brain endothelial cells can be targeted and opened in reversible manner by peptides, which significantly increases permeability of tracer molecules including EBA (Bocsik et al. 2016).

In a cooperation with German partners we tested drug-enhancer peptides designed based on the first extracellular loop of claudin-5, the major tight junction protein at the BBB. Peptidomimetics C5C2 and its derivatives, had nanomolar affinity to claudin-5 and size-selectively (<40 kDa) and reversibly (12–48 h) increased the permeability of brain endothelial cell layers. The claudin-5-derived peptide C5C2 also decreased paracellular tightness and opened interendothelial tight junctions in our triple co-culture BBB model (Fig. 18). Filter-grown primary rat brain endothelial cells co-cultured with pericytes and glial cells were treated with 300 μ M C5C2 or a claudin-2-derived control peptide (C2C2) for 24 hours. Decrease of the transcellular electrical resistance after treatment with C5C2 was observed compared to cells treated with medium without peptide, indicating opening of the junctions. The control peptide did not alter the resistance. Transmission electron microscopy verified the opening of interendothelial tight junctions in cells treated with C5C2. No change was seen in brain endothelial cells cultured without peptide or treated with control peptide (Fig. 18.).

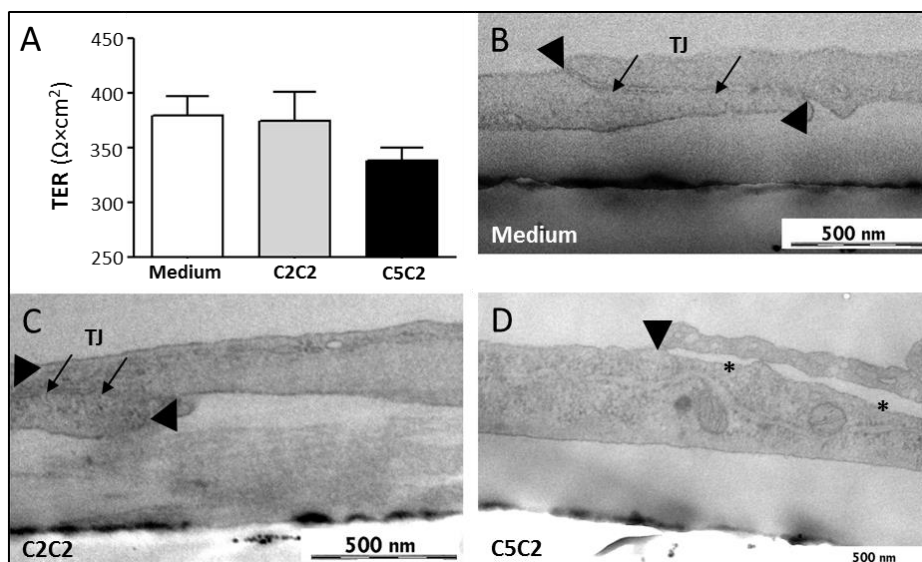


Fig. 18. (A) The effect of C5C2 (300 μM) or a claudin-2-derived control peptide (C2C2) on transcellular electrical resistance (TER) after 24 hours incubation. $n=3$, mean \pm SD, *, $P<0.05$, ANOVA and Dunnett test. (B-C) Transmission electron microscopy revealed an opening of interendothelial tight junctions (asterisks) in cells treated with (D) C5C2 in comparison to cells (B) cultured without peptide or (C) with control peptide; \uparrow , tight junction, TJ; \blacktriangle , beginning and end of interendothelial tight junctions (TJ).

Summary and importance of the results

Novel drug delivery systems that are able to cross or open the BBB in a controlled and non-invasive manner may improve the therapy of CNS diseases. Specific targeting can be achieved through exploiting the physiological transport pathways of the BBB. Despite the abundance of carrier mediated transporters at the BBB this physiological pathway is still not fully exploited for drug delivery. In our study we selected ligands for the endogenous nutrient transporters of brain endothelium to target solid and vesicular nanoparticles. We identified biotin as a potential BBB targeting ligand and verified the expression of its transporter SLC5A6 in brain endothelial cells. Functionalization of solid nanoparticles with biotin increased the uptake and the transfer of nanoparticles across brain endothelial cells. We used glutathione as a reference ligand and confirmed its effectiveness as a BBB targeting vector. We discovered that alanin both alone, and combined with glutathione as double targeted ligands on the surface of vesicular nanoparticles were efficient to deliver a large molecular cargo across the BBB in cell culture and animal experiments. We identified that endocytosis, membrane fusion and brain endothelial surface charge all contribute to the cellular uptake mechanisms of nanocarriers. The novel claudin-5 peptidomimetic C5C2 transiently opened the BBB and improved drug penetration to brain, indicating that targeting tight junction proteins of brain endothelial cells constitute a promising approach as drug delivery system. Based on our observations nutrient transporter ligands biotin and alanin may have a potential to be used as BBB targeting molecules on nanoparticles. Combination of different targeting ligands could be a novel way to increase drug delivery to brain by nanoparticles.

References

- Abbott NJ, Patabendige AA, Dolman DE, *et al.* Structure and function of the blood-brain barrier. *Neurobiol Dis.* 2010;37(1):13-25.
- Campos-Bedolla P, Walter FR, Veszelka S, Deli MA. Role of the blood-brain barrier in the nutrition of the central nervous system. *Arch Med Res.* 2014 Nov;45(8):610-38.
- Bocsik A, Walter FR, Gyebrovski A, Fülöp L, Blasig I, Dabrowski S, Ötvös F, Tóth A, Rákhely G, Veszelka S, Vastag M, Szabó-Révész P, Deli MA. Reversible Opening of Intercellular Junctions of Intestinal Epithelial and Brain Endothelial Cells With Tight Junction Modulator Peptides. *J Pharm Sci.* 2016 Feb;105(2):754-765.
- Gaillard PJ, Appeldoorn CC, Dorland R, van Kregten J, Manca F, Vugts DJ, Windhorst B, van Dongen GA, de Vries HE, Maussang D, van Tellingen O. Pharmacokinetics, brain delivery, and efficacy in brain tumor-bearing mice of glutathione pegylated liposomal doxorubicin (2B3-101). *PLoS One.* 2014 Jan 8;9(1):e82331.
- Hervé F, Ghinea N, Scherrmann JM. CNS delivery via adsorptive transcytosis. *AAPS J.* 2008 Sep;10(3):455-72.
- Kiss L, Hellinger É, Pilbat AM, Kittel Á, Török Z, Füredi A, Szakács G, Veszelka S, Sipos P, Ózsvári B, Puskás LG, Vastag M, Szabó-Révész P, Deli MA. Sucrose esters increase drug penetration, but do not inhibit p-glycoprotein in caco-2 intestinal epithelial cells. *J Pharm Sci.* 2014 Oct;103(10):3107-19.
- Neuwelt EA, Bauer B, Fahlke C, *et al.* Engaging neuroscience to advance translational research in brain barrier biology. *Nat Rev Neurosci.* 2011;12(3):169-82.
- Pardridge WM. Blood-brain barrier endogenous transporters as therapeutic targets: a new model for small molecule CNS drug discovery. *Expert Opin Ther Targets.* 2015;19(8):1059-72.
- Pardridge WM. Drug transport across the blood-brain barrier. *J Cereb Blood Flow Metab.* 2012;32(11):1959-72.
- Ribeiro MM, Domingues MM, Freire JM, Santos NC, Castanho MA. Translocating the blood-brain barrier using electrostatics. *Front Cell Neurosci.* 2012 Oct 11;6:44.
- Weksler B, Romero IA, Couraud PO. The hCMEC/D3 cell line as a model of the human blood brain barrier. *Fluids Barriers CNS.* 2013 Mar 26;10(1):16.